

Accepted Manuscript

Title: The transient start-up response of a universal exhaust gas oxygen sensor to investigate the Nernst equation in platinum/zirconia cells

Author: J.A. Harris N. Collings

PII: S0925-4005(15)00784-4
DOI: <http://dx.doi.org/doi:10.1016/j.snb.2015.05.131>
Reference: SNB 18586

To appear in: *Sensors and Actuators B*

Received date: 20-10-2014
Revised date: 19-5-2015
Accepted date: 31-5-2015

Please cite this article as: J.A. Harris, N. Collings, The transient start-up response of a universal exhaust gas oxygen sensor to investigate the Nernst equation in platinum/zirconia cells, *Sensors & Actuators: B. Chemical* (2015), <http://dx.doi.org/10.1016/j.snb.2015.05.131>

This is a PDF file of an unedited manuscript that has been accepted for publication. As a service to our customers we are providing this early version of the manuscript. The manuscript will undergo copyediting, typesetting, and review of the resulting proof before it is published in its final form. Please note that during the production process errors may be discovered which could affect the content, and all legal disclaimers that apply to the journal pertain.



The transient start-up response of a universal exhaust
gas oxygen sensor to investigate the Nernst equation in
platinum/zirconia cells

J.A. Harris*, N. Collings

Department of Engineering, University of Cambridge, Cambridge, CB2 1RD, UK

Abstract

The universal exhaust gas oxygen sensor (UEGO) is a device used to infer the combustion air-to-fuel ratio of an internal combustion engine by sampling the exhaust gas. The sensor operates using a feedback system to maintain a specified internal condition, and measures the oxygen current required for this. While the steady state operation of the sensor is reasonably well-understood - dominated as it is by the diffusion of gas species - the factors influencing the transient response are not so clear.

In this paper a numerical model of a sensor is compared to experimental data. By examining the effect of the inclusion of different aspects into the model, it becomes clear that it is necessary to account for the influence of gaseous species adsorbing onto surfaces, as well as the more traditional approach based on oxygen partial pressure, to correctly capture the transient response of a sensor containing a Pt|YSZ|Pt cell.

Keywords: UEGO, transient, adsorption

1. Introduction

The universal exhaust gas oxygen (UEGO) sensor has become a commonplace as a method to determine the non-dimensional air-fuel ratio (λ) of IC

*Corresponding author
Email address: jah213@cam.ac.uk (J.A. Harris)

engines, and may form a part of a feedback control system of the engine. Its usage has increased in order to help meet increasingly stringent emission regulations for both diesel and gasoline engines. A related sensor, the so called 'HEGO' (Heated Exhaust Gas Oxygen) sensor - also known as a 'narrowband' or 'switch-type' - is of a simpler design, has been used for significantly longer, and is an essential component of most gasoline engines where emission regulations exist. This sensor gives a virtually binary output, depending upon whether the exhaust is a product of rich or lean combustion. However the UEGO, also known as a 'wideband' sensor, gives a measure of how rich or lean the combustion is. Under steady conditions the UEGO output is dominated by the diffusion of gases, and this aspect has been modelled previously [1].

Though designs vary considerably, the schematic of a common type is shown in figure 1. The key components of a UEGO are the 'reference cell', the 'pump cell', the measurement cavity, and the 'diffusion barrier' built mainly from layers of yttria-stabilised-zirconia (YSZ). At elevated temperature YSZ is a good conductor of oxygen ions. The method of operation is based on achieving a constant oxygen partial pressure in the measurement cavity. The desired state is identified via the Nernst potential generated by the reference cell - if the potential is lower than the reference voltage (i.e. the oxygen partial pressure is too high), then the feedback circuit corrects this by causing the pump cell to extract more oxygen from the measurement cavity. The reverse happens if the reference cell potential is higher than the reference voltage. The pumped oxygen passes through the pump cell in the form of O^{2-} ions. The actual rate of oxygen pumping required is determined by the diffusion of gases through the diffusion barrier from the sample gas to the measurement cavity. Under rich exhaust conditions ($\lambda < 1$) an excess of hydrogen and carbon monoxide diffuse into the cavity, the oxygen required to oxidise these is produced by the breakdown of water and carbon dioxide on the side of the pump cell exposed to the sample gas and pumped into the cavity. Under lean exhaust conditions ($\lambda > 1$) oxygen gas diffuses through the diffusion barrier, and is pumped out of the cavity. The quantity of O^{2-} pumped is thus an indication of the leanness/richness of the

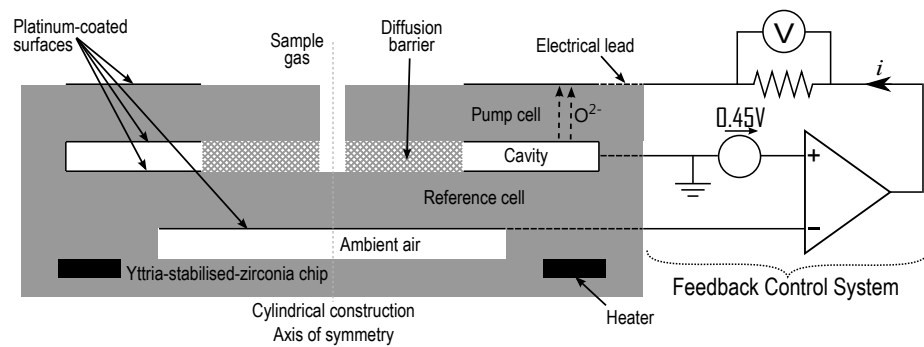


Figure 1: A schematic cross section of a UEGO, indicating the location of the built in heater, the location of platinum electrode surfaces, and the feedback control system. The ‘cavity’ electrodes are connected to ground, it is this ground that pump and reference cell potentials are measured relative to. An additional feedback circuit exists to control the power applied to the heating elements, holding the sensor at a constant temperature.

sample gas. The sensor design considered here is the Bosch LSU4.2, further references to ‘UEGO’ refer to this type.

Though under steady conditions the UEGO response is determined by the diffusion barrier, under transient conditions this is not true. This is clearly seen in the sensor response to a sample gas crossing stoichiometry [2]. In this case the Nernstian potential of the pump cell changes very rapidly, and the sensor output departs from the value predicted by gas diffusion through the barrier. To explore this further, this paper will focus on the transient response of the UEGO in ambient air, and examine the mechanism by which the voltage across the reference cell is generated.

2. Background Theory

2.1. Pressure Based Nernst Equation

As discussed above, the feedback system within the UEGO which causes a flow of O^{2-} through the YSZ pump cell, is determined by the voltage across the reference cell. The feedback system is designed to maintain this reference voltage at 0.45 V, which corresponds to a stoichiometric gas mixture, i.e. $\lambda = 1$.

The traditional mechanism for this voltage generation, as seen in [1, 3, 4], is considered to be purely a function of the partial pressures of oxygen in the measurement cavity (cav) and reference gas (ref), the so-called Nernst potential.

$$E = \frac{\mathfrak{R}T}{4F} \ln \left(\frac{p_{O_2, \text{ref}}}{p_{O_2, \text{cav}}} \right) \quad (1)$$

Here \mathfrak{R} is the universal molar gas constant, T the absolute temperature, F Faraday's constant, and p_{O_2} the partial pressure of oxygen. The factor of 4 arises from the fact that an oxygen molecule ionises to form two O^{2-} , therefore the negative charge associated with ionisation is 4. This equation is derived from the difference in entropy, S , between the two gas compositions, following the derivation found in [5] and beginning with Boltzmann's equation $S = k_B \ln \Omega$ (k_B being the Boltzmann constant). The number of states available Ω is considered inversely proportional to the pressure of the gas. The equation for Gibbs free energy G , noting that the enthalpy change across the reference cell (ΔH) is zero because the same species is being considered, can also be linked to the electromotive potential E of a reaction including the number of electrons involved z and the elementary charge e : $\Delta G = \Delta H - T\Delta S = -zeE$. Combining these we have

$$E = \frac{-T}{ze} \left(k_B \ln \left(\frac{1}{p_{O_2, \text{ref}}} \right) - k_B \ln \left(\frac{1}{p_{O_2, \text{cav}}} \right) \right) \quad (2)$$

Using the fact that in this case $z = 4$ and $k_B/e = \mathfrak{R}/F$ leads directly to equation (1) is reached. The reference voltage being set to 0.45V and the reference gas being ambient air this leads to a conclusion that the partial pressure of oxygen within the measurement cavity is approximately 2.9×10^{-5} Pa.

2.2. Diffusion/Drift Based Nernst Equation

Yttria-stabilised-zirconia is a ceramic composed of the elements yttrium, zirconium, and oxygen. Yttrium and zirconium are transition metals of adjacent atomic number, meaning they are of similar atomic size but differing ionisation states. The similar size means yttrium can be inserted, or 'doped', into the lattice structure of zirconium oxide and the different stable ionic states lead to

a vacancy in the lattice where an oxygen atom would normally sit. The vacancies are not restricted to remain next to the dopant ion as electrical neutrality is maintained wherever a vacancy lies. Oxygen conduction is achieved by O^{2-} swapping location within the lattice with a vacancy (denoted $V_O^{\circ\circ}$), and this ability for movement results in the possibility of diffusion if there is a gradient in the concentration of vacancies $[V_O^{\circ\circ}]$ or electrical drift should a voltage gradient act upon the ions. Vacancies can be considered to have a charge of +2, as although there is nothing present it is a location a 2- ion could sit, and in the analysis of Brailsford et al. [6] it is the vacancies that are examined.

Vacancy flux \mathbf{J} due to diffusion is simply proportional to the diffusivity of vacancies \mathcal{D} and the concentration gradient, $\mathbf{J}_{\text{diff}} = -\mathcal{D}\nabla[V_O^{\circ\circ}]$. The flux due to an applied electric field \mathbf{E} is dependent on the field, the local concentration of vacancies to be effected, and the mobility μ_q of vacancies - a measure of the terminal velocity when an electric field acts on an ion. $\mathbf{J}_{\text{elec}} = \mu_q[V_O^{\circ\circ}]\mathbf{E}$

The Einstein-Smoluchowski relationship enables the two sources of vacancy flux to be combined, relating the mobility to diffusivity: $\mu_q = ze\mathcal{D}/k_B T$. That these values are related is no surprise as they are both measures of how ions (or vacancies in this case) move through a lattice. There is no current flow through the reference cell, so the combined diffusion and electrically driven fluxes must cancel.

$$0 = -\mathcal{D}\nabla[V_O^{\circ\circ}] + \mu_q[V_O^{\circ\circ}]\mathbf{E} \quad (3a)$$

$$\Rightarrow \mathcal{D}\nabla[V_O^{\circ\circ}] = \frac{ze\mathcal{D}}{k_B T}[V_O^{\circ\circ}]\mathbf{E} \quad (3b)$$

Simplifying to a single dimension x_1 , and giving the electric field as the gradient of a potential field so $\mathbf{E} = \nabla E = dE/dx_1$ the component of direction can be cancelled allowing an integral to be taken between vacancy concentrations and the potential between the two.

$$\int \frac{d[V_O^{\circ\circ}]}{[V_O^{\circ\circ}]} = \frac{ze}{k_B T} \int dE \quad (3c)$$

As in this case the charge on each ion z is equal to two, leaving a subtly different version of equation (1) based on the vacancy concentration in the YSZ instead

of external partial pressures.

$$E = \frac{\mathcal{R}T}{2F} \ln \left(\frac{[V_O^{\circ\circ}]_{\text{cav}}}{[V_O^{\circ\circ}]_{\text{ref}}} \right) \quad (3d)$$

The form taken by drift/diffusion allows simple addition of a voltage due to passing a current, an additional linear electric field (as one would expect for a current passing through a resistor) allows a net flow of ions. Therefore across the pump cell of a UEGO the voltage measured is a combination of equation (3d) and a term $i_p R_{YSZ}$, the pump current i_p and the apparent pump cell resistance R_{YSZ} .

2.3. Platinum|Yttria-Stabilised-Zirconia

The interaction between the platinum surface and YSZ substrate was examined by Auckenthaler et al. [7] for a similar application in the HEGO type sensor. As described in [8] the electrode kinetics of the system is dominated by the condition of the surface and the point it meets the electrolyte at the ‘triple-phase-boundary’. The concentration of vacancies in the YSZ in contact with the platinum was considered to be dependent on the oxygen adsorbed upon the platinum surface. It is recognised [9, 10] that a platinum surface has defined sites at which an oxygen molecule or atom can adsorb onto the surface - the fraction of sites occupied by an oxygen ‘adatom’ signified θ . The full details of oxygen adsorption are not presented here, full details of the precursor mediated adsorption (as initially an oxygen molecule attaches to a vacant site before splitting into two oxygen adatoms) can be found in [11]. The values for surface bond strengths within the model are taken from the work of Mitterdorfer and Gauckler [12] based on electrode impedance spectroscopy. The adsorption of oxygen onto the surface is dependant on the flux of oxygen molecules upon the surface, the probability of a molecule sticking to the surface, and the fraction of surface sites that remain vacant ($1 - \theta$). Desorption from the surface depends on the fraction of sites occupied, and the proportion with sufficient vibrational energy to break the bond to the surface (i.e. desorption increases with temperature). The existence of a precursor state (adsorbed molecular oxygen) leads to a rate

dependence proportional to $\theta^2 / (1 + k(1 - \theta))$, where k is the ratio of adsorbed molecules that split into adatoms to those that desorb from the surface.

The HEGO model in [7] considers all species found within an internal combustion engine exhaust, but for the current work the only relevant species are oxygen and nitrogen. The construction of the sensor, in particular the quantity of platinum close enough to the YSZ to count as part of a ‘triple-phase-boundary’, and the adsorbed oxygen concentration gradient led to the conclusion that the concentration of vacancies within the YSZ at the boundary with the platinum is proportional to the value θ^{-4} . It is by using this substitution an alternative calculation for the reference cell voltage can be achieved.

$$E = \frac{\mathfrak{R}T}{2F} \ln \left(\frac{\theta_{\text{ref}}^4}{\theta_{\text{cav}}^4} \right) \quad (4)$$

3. Experimental Procedure and Results

During experiments the UEGO is held at a temperature of 750°C, a temperature where the YSZ will freely conduct oxygen ions. The sensor temperature is maintained using a feedback system. The electrical resistance of the reference cell is interrogated by injecting a small spike of current and measuring the corresponding change in cell potential. These injections are small enough and infrequent enough to have negligible effect on the operation of the sensor. The resistance of the YSZ is interpreted via Ohm’s Law, and is a known function of temperature. This means the sensor heating circuit can be controlled via a feedback circuit (not shown in figure 1) to ensure the reference cell is maintained at an electrical resistance corresponding to the desired operating temperature. When the temperature feedback system was required to be briefly detached, the sensor was monitored for a prolonged period to establish the stable heater supply power, and this level was then held for the duration of the disconnect.

The first experiment undertaken was to measure the apparent resistance of the UEGO pump cell at varying pump currents in steady state. The feedback control circuit was disconnected from the UEGO, and replaced by a constant current source attached to the pump cell, and an oscilloscope connected to both

pump and reference cells. The measurements taken are shown in figure 2, along with a prediction of the apparent resistance - that is the difference between pump and reference cell voltages divided by applied pump current - allowing for the influence of the 'Seebeck effect', i.e. the small voltage induced across the cells by temperature gradients within the UEGO which adds an artificial component to the difference in cell voltages. This temperature gradient is estimated by the power delivered to the heater circuit and further refined by a fit to the data. Also shown is the calculated partial pressure of oxygen within the cavity based on the model provided by [1]. The contribution of the Seebeck effect is 10.4 mV, which using an associated Seebeck coefficient of 0.438 mV/K[13] corresponds to a temperature difference across the cell of about 25 K - which is not excessive when the high temperature of the sensor compared to its ambient surroundings and the power drawn by the heater circuit are considered. The departure from the apparent resistance expected from the Seebeck model becomes clear as the partial pressure of oxygen within the cavity becomes very small. The range of pump currents applied did not exceed the rate at which oxygen could be supplied from the diffusion barrier. Applying a *continuous* pump current above 4 mA leads to reduction of the YSZ within seconds due to the diffusion barrier preventing additional flow leading to an oxygen deficiency within the cavity, signified by a jump in measured reference and pump cell voltages. To prevent this undesirable effect the UEGO was always protected by either the feedback circuit or a relay designed to cut the pump current once the reference cell voltage exceeded 0.45 V.

For the second test the feedback circuit was reapplied but the pump current disconnected. A resistor was also added to the pump cell circuit, and measuring the voltage across this allowed the applied pump current to be calculated. The removal of the pump current allowed the cavity to equalise with ambient conditions, therefore the oxygen concentration was ambient throughout the sensor. The pump current was then reconnected, while measuring the voltage across reference and pump cells (figure 3). The driving op-amp for the feedback circuit was unable to produce more than approximately 8 mA, but due to the restric-

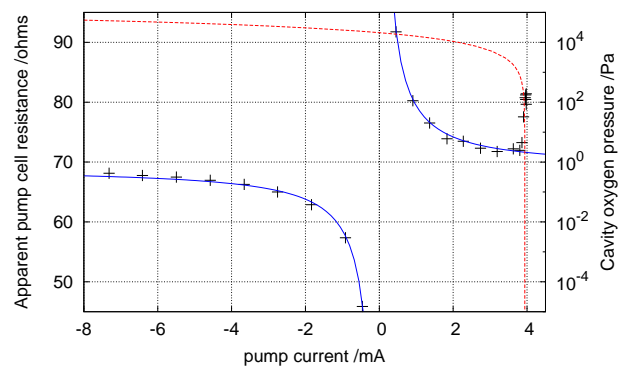


Figure 2: The apparent resistance of the pump cell and the steady state cavity oxygen partial pressure. The departure of the apparent resistance from a 'Seebeck model' clearly occurs as the O_2 pressure drops towards zero.

tion provided by the diffusion barrier this was more than sufficient to reduce the oxygen concentration within the cavity to very low levels. The initial jump in the reference cell voltage seen when the current is connected at $t = 0$ is due to the earth connection from the cavity leadout having a non-negligible resistance, the jump in pump cell voltage is from the pump cell YSZ resistance as well as the cavity earth connection.

The simplest model of the UEGO, taking the Nernst potential as in equation (1), would suggest that the voltages across reference and pump cells should differ by just the product of pump current and pump cell YSZ resistance. What is in fact observed during the initial 8 mA pump current application is that the difference between voltages increases as oxygen is pumped out of the cavity reducing the oxygen partial pressure from ambient to the operating level. After this initial evacuation period the voltage difference decreases in line with the reducing pump current.

The final test had the feedback circuit removed and a constant current source attached, again initially disconnecting the pump current to allow the cavity to reach ambient conditions. The pump current was varied for separate current-

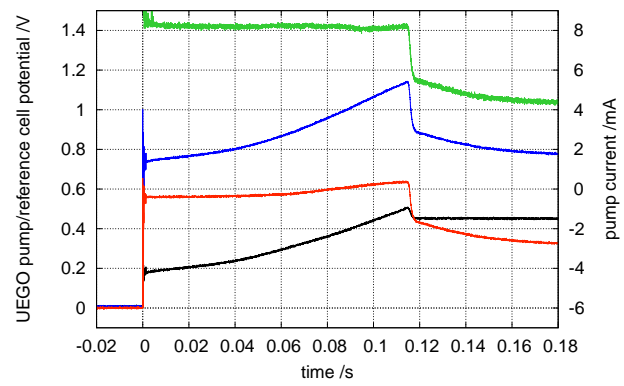


Figure 3: Plot of the Reference Cell, UEGO Cell, Difference, and Pump Current as the feedback current circuit is closed. UEGO in ambient air at 750°C, circuit closed at $t = 0$. This shows the initial period of a maximum steady pump current extracting oxygen from the UEGO cavity, and once the reference cell voltage has reached the setpoint of 0.45V the pump current reduces purely to match the oxygen flow provided by the diffusion barrier. The method of measuring the pump current means it is shown as high before $t = 0$ when it is in fact zero.

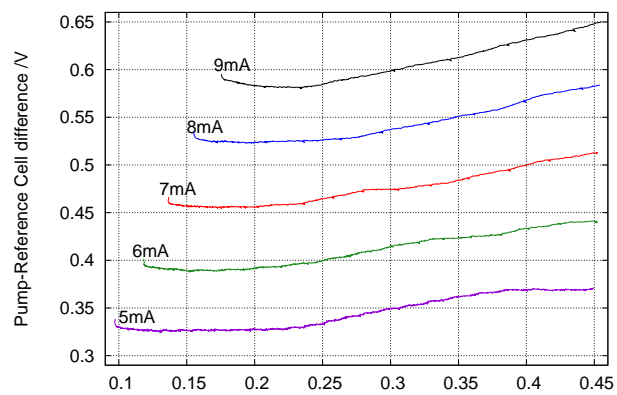


Figure 4: The difference between pump cell voltage and reference cell voltage as a function of the reference cell voltage, plotted for pump currents between 5mA and 9mA.

reconnection tests, and the higher the pump current, the more rapidly the cavity is evacuated. The time taken for the reference voltage to reach 0.45 V is not constant, so the difference between pump and reference cell voltages are instead plotted against the reference cell voltage in figure 4. Using the reference cell voltage instead of time as a measure of how the cavity oxygen partial pressure has reduced, it can again be seen that the voltage difference does not remain constant as the cavity is evacuated. The similarity in profiles, the voltage difference rising as a function of reference cell voltage and not of the pump current used, suggests the dominant cause of the difference is linked to the reference cell potential more than it is linked to the size of the current and associated reaction overpotential.

Experiments were repeated on a number of days, different ambient conditions (i.e. variable humidity and temperature) were not seen to have an effect on the UEGO behaviour. The geometry of the sensor was established by cutting the YSZ chip, through a plane cutting the centre of the axis of cylindrical symmetry. A SEM image was taken and used to measure the dimensions of the sensor. The diffusion barrier was between radii of approximately 0.11 mm and 0.81 mm, while the gas cavity then extending out to ~ 1.45 mm. The height of the diffusion

barrier and cavity was $\sim 30 \mu\text{m}$.

4. Modelling

A numerical model of the UEGO requires at least three components; a representation of the diffusion barrier, determination of the voltage according to equations (1) or (3d), and a link between the the barrier and the voltage determination. If the voltage were related only to the oxygen partial pressure this link is as simple as integrating the flows of oxygen into the cavity from the diffusion barrier and the quantity pumped out. If, on the other hand, the voltage is determined using the diffusion/drift equation, the link also includes the adsorption of gaseous species onto the platinum electrodes for interaction with the YSZ. Here we restrict ourselves to considering an N_2/O_2 system.

4.1. Diffusion Barrier

As shown in [1], the Stefan-Maxwell equations provide an excellent steady-state description of the diffusion barrier characteristics, though the diffusion problem is made more complex by the fact the diffusion is a mixed free-molecular/continuum process, due to the gas mean-free-path being of a similar scale to the pore size within the diffusion barrier. For the transient case here the barrier was modelled as a series of rings all in quasi-equilibrium. A simplification was made to the prediction of pressure loss across the barrier, which is a function of the average molecular mass of (net) moving particles. This was replaced by the molecular mass of oxygen, as only oxygen moves under steady state and in a situation where instead it was purely nitrogen moving the error would be at most 15% (as $1 - M_{N_2}/M_{O_2} < 15\%$).

Working in molecular concentrations c rather than pressures, but otherwise using the notation from [1], this leads to a total molecular flux J_{tot} of

$$J_{\text{tot}} = \frac{-\varepsilon}{\tau^2} \frac{\mathfrak{R}T}{M_{O_2}^{1/2}} \frac{1}{A_A} \frac{dc}{dr} \quad (5)$$

Of this total flow the component which is oxygen is J_{O_2}

$$J_{O_2} = \frac{\frac{X_{O_2} J_{tot}}{D_{N_2, O_2}} - \frac{\varepsilon}{r^2} c \frac{dX_{O_2}}{dr}}{\frac{X_{O_2}}{D_{N_2, O_2}} + \frac{X_{N_2}}{D_{O_2, N_2}}} \quad (6)$$

Finally, the fluxes can be integrated to find the concentrations of each species throughout the barrier.

$$c_s = \int \frac{-1}{\varepsilon r} \frac{d(rJ_s)}{dr} dt \quad (7)$$

This transient model of the diffusion barrier settles as $t \rightarrow \infty$ to match the radial oxygen partial pressure distribution and molecular flux as calculated using a full computational model from [1]. This ‘transient’ (although quasi-equilibrium) model would become far more complex if further species were to be introduced.

4.2. Oxygen Adsorption

The precursor-mediated-adsorption model from Mitterdorfer and Gauckler [12] can be used to calculate the rate of oxygen extraction from the cavity, as each molecule sticking to the surface is taken out of the gas. The assumption that almost entirely all surface adsorbed oxygen is atomic instead of molecular is valid due to the high temperature (above 300 K) of the UEGO. We take the number of discrete adsorption sites as Γ , the flux of O_2 onto a surface \mathcal{F}_{O_2} and the probability of sticking ζ , the value k_d is rate constant for adatoms combining to molecular adsorbed oxygen, and k the ratio of rate of decomposition of adsorbed molecular oxygen to the rate of molecular oxygen desorption. The assumption of negligible molecular adsorbed oxygen means the quantity can be assumed to be in quasi-equilibrium, so the rate of change of surface coverage θ is given by

$$\frac{d\theta}{dt} = \frac{\mathcal{F}_{O_2}}{\Gamma} \frac{2\zeta k}{1+k(1-\theta)} (1-\theta)^2 - \frac{2k_d \Gamma}{1+k(1-\theta)} \theta^2 \quad (8)$$

On the pump cell surface adsorbed oxygen is subtracted from the platinum at a rate equivalent to the pump current transporting oxygen ions, and added to the pump cell surface interacting with air.

The area of platinum electrode available is much greater than the pure geometric area due to the porosity of the electrode. A rough approximation might be that the electrode is formed of spheres with diameter d , and then the ratio of actual platinum area to geometric (2-D) area in a layer of height h_{Pt} is

$$A_{rat} = (6\pi h_{Pt}) / (d\sqrt{18}) \quad (9)$$

Using data from Melo et al. [14] platinum layers between $0.05\mu\text{m}$ and $0.2\mu\text{m}$ lead to a value for the area ratio between 15 and 40. Additionally a term for diffusion between cavity surfaces is included, this term allowing for the contact between the electrodes at the cavity outer radius with an separation equal to the cavity height. The surface diffusion D_s value is taken to be constant in the absence of contrary information. The driving force for this may not be diffusion, but an effect of electric fields within the UEGO acting upon the O^{2-} .

4.3. Voltages

The voltages simulated for the reference and pump cells are calculated according to equation (4), plus the effect of resistances within the UEGO. The reference cell voltage is increased by a factor $i_{pump}R_{leadout}$, while the pump cell includes both the leadout resistance and a combined lead/ionic conduction term.

5. Simulations

Use of the model as described above to mimic the switch-on test in figure 3 produces figure 5. The value A_{rat} used was 25, and the value of D_s set at $10^{-4} \text{m}^2\text{s}^{-1}$. The similarities between experimental and simulated situations are clear, both take approximately 0.1s to reach a reference cell voltage of 0.45 V and at the time this reference cell voltage is achieved, the pump cell voltage is approximately equal to 1.1 V. In the experimental equivalent the reference voltage actually exceeded the 0.45 V set point briefly, this isn't shown in the simulation due to the 'perfect' nature of the simulated feedback control. The

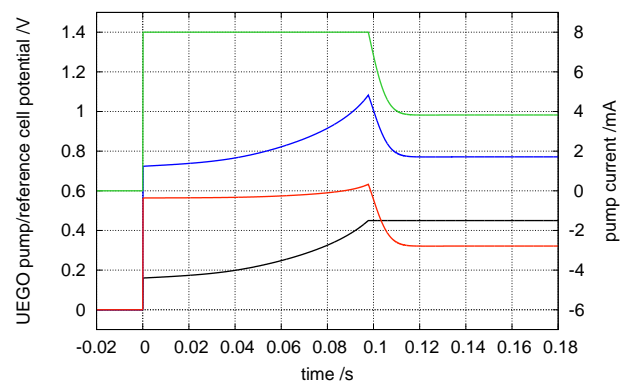


Figure 5: Results of a feedback control system for a UEGO pump. The graph plots UEGO pump/reference cell potential (V) on the left y-axis (0 to 1.4) and pump current (mA) on the right y-axis (-6 to 8) against time (s) on the x-axis (-0.02 to 0.18). Three data series are shown: Reference Cell (black line), Pump Cell (blue line), and Pump Current (green line). The Reference Cell potential starts at 0V and steps up to approximately 0.6V at t=0. The Pump Cell potential starts at 0V and rises to approximately 1.1V at t=0.1s, then levels off. The Pump Current starts at 0mA and steps up to approximately 4mA at t=0, then levels off. All signals show a transient response between t=0 and t=0.1s.

pump current is also seen to ‘tail-off’ after the reference voltage is achieved in a similar manner to the experiment. Matching the experiment shown in figure 4, at higher pump currents the simulation shows an excellent agreement (the voltage difference is slightly high throughout, suggesting a small overestimate in the pump cell resistance). The difference between pump and reference cell voltages increases with the reference cell potential as per the experimental data, but the simulation for a 5 mA pump current shows a slightly worse match as it does not replicate the slight ‘leveling-off’ of the voltage difference seen in the real sensor as the reference voltage increased. The reason for the discrepancy is unclear, but at the lowest current any mechanism that acts to equalise the cell voltages will have a greater effect due to the slower rate of voltage change. The similarity between figures 4 and 6, while the simulation contains no accounting for an overpotential due to the current, suggests that the transfer of oxygen from the platinum surface to the YSZ is not a rate limiting step.

For contrast, a simulation was run extracting oxygen from the cavity at exactly the rate equivalent to the pump current - i.e. the platinum electrodes and surface adsorption kinetics were not present as a ‘buffer’ between the gases within the cavity and the process of pumping oxygen ions away from the cavity.

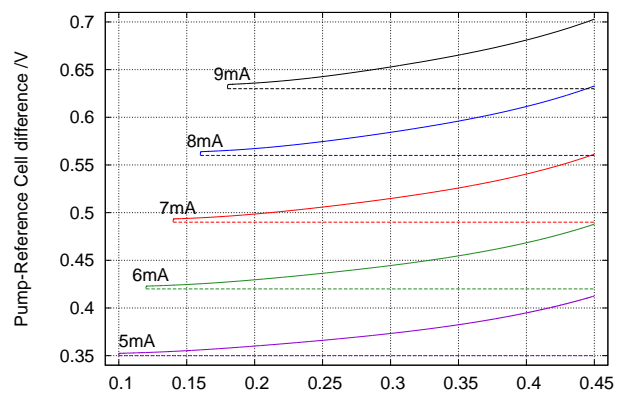


Figure 6: The simulated result for the surface adsorption model (solid lines) to figure 4. The dotted lines show the result for an assumed constant pump cell resistance and both cell voltages purely a function of the oxygen partial pressure on either side.

Without any representation of electrodes the voltages within the sensor can only be calculated using the oxygen partial pressure as used in equation (1) (although still including the effect of lead and pump cell resistances). Figure 7 shows that although the initial response is similar - the pump and reference cell voltages slowly increase with time as the oxygen is removed from the cavity - the voltage spikes rapidly after 0.027 s. The simulation broke down at this point, as the voltages rise rapidly with the oxygen partial pressure dropping away. This simulation is certainly a poorer match to experimental data than the surface adsorption model.

5.1. Effect of area ratio and surface diffusivity

The estimated value of platinum surface area has an important effect on the simulation output. The two dimensional geometric area is $4.54 \times 10^{-6} \text{ m}^2$, taken from measurement of SEM images of the cavity; the area ratio is not so easily measured, so the effect of varying this parameter upon the simulation is examined here.

For a fixed pump current, the rate of change in fractional coverage θ is

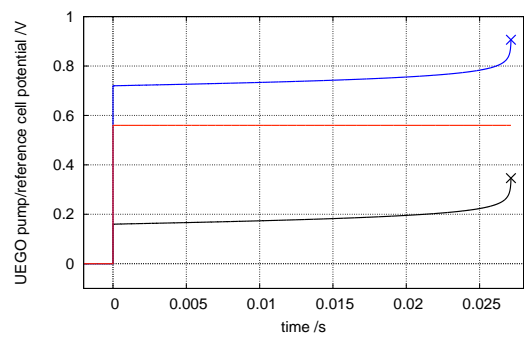


Figure 7: A simulation of pumping oxygen from the UEGO cavity at a rate of $2.073 \times 10^{-11} \text{ kmol.s}^{-1}$, equivalent to 8mA, and calculating the voltage using the Nernst equation based upon the ratio of partial pressures either side of the pump and reference cells.

reduced by a high value for the area ratio .

$$\left(\frac{d\theta}{dt}\right)_{\text{pumping}} \propto \frac{1}{A_{\text{Pt}}} \quad (10)$$

The removal of gaseous oxygen is driven by the surface coverage dropping below the equilibrium value, caused by the pump current. This implies that a high platinum surface area ratio would lead to a longer startup transient, due to the removal of oxygen from the cavity being slowed. However, an increase in area ratio also provides an increased number of surface sites available for the adsorption of gaseous oxygen.

$$\left(\frac{dp_{\text{O}_2}}{dt}\right)_{\text{adsorption}} \propto A_{\text{Pt}} \quad (11)$$

The higher number of molecules being absorbed causes a greater rate of oxygen extraction from the cavity. The balance between these two contrasting effects is examined by measuring the time taken for the simulation to reach a reference cell voltage of 0.45 V, with the results shown in figure 8. A large range is shown, but the point at which the simulation matches the experimental value of $\approx 0.1 \text{ s}$ coincides with an area ratio of approximately 25 - a value within the range predicted by equation (9) and the data from [14]. It is perhaps surprising how

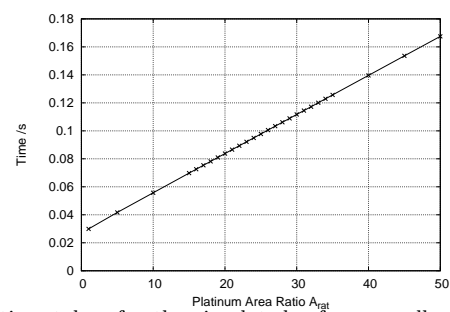


Figure 8: The time taken for the simulated reference cell voltage to reach 0.45V due to a constant 8mA pump current as a function of the platinum electrolyte area ratio A_{rat} .

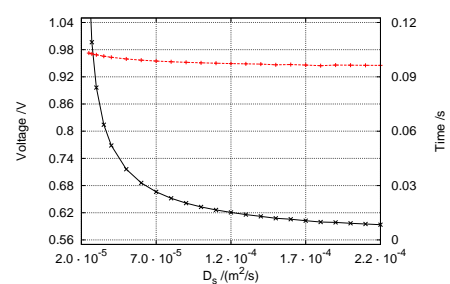


Figure 9: The effect of varying the value D_s , showing the difference in voltages measured at a reference cell potential of 0.45 V, and the small influence on the time taken to reach this point.

linear the plot is, as the reaction time decreases it might be expected to see more influence from the diffusion barrier's transient response.

The D_s value used is somewhat empirically fitted, as it acts as a damping force between the two surface coverage fractions in the cavity electrode surfaces. The value influences the difference in pump and reference cell voltages, as shown in figure 9, and although there is a small effect on the time taken for the target reference cell voltage of 0.45 V to be reached, it is predominantly the voltage differences that are influenced. The value used in simulations does not match published data for diffusion of surface adsorbed oxygen on platinum by several orders of magnitude, giving greater probability to the idea that the process is actually driven by a mechanism other than a pure concentration gradient.

6. Conclusion

It is clear that with a low oxygen partial pressure in the UEGO cavity there is an apparent increase in the electrical resistance of the pump cell, meeting the expectation that the mechanism is not as simple as a pure resistance. This work has considered oxygen adsorption on platinum surfaces as a dominating mechanism in this more complex system. The transient behaviour due to switching the UEGO feedback system on provides a prolonged response, suitable for comparing models of the voltage defining mechanism in the reference cell. A surface adsorption model, similar to that previously applied successfully to a HEGO sensor, appears to provide a good first approximation for the UEGO behaviour. The applied model, although featuring some empirically fitted values, provides a superior match to experimental data than the more traditionally used method for calculating the reference cell voltages using pure oxygen partial pressures.

The conditions used in these experiments were selected because of the relatively long time the transient characteristics exist, and the relatively simple relationship between adsorption of oxygen and voltage generation. A natural extension of this work would be to include reducing species such as carbon monoxide and hydrogen in the diffusion, adsorption, and voltage generation models. Additionally it would be required to include the oxidation of these species as catalysed by the platinum surfaces. This would allow the simulated UEGO to be used when predicting situations involving a rich or even trans-stoichiometric exhaust gas composition.

References

- [1] N. Collings, K. Hegarty, T. Ramsander, Steady-state modelling of the universal exhaust gas oxygen (UEGO) sensor, *Measurement Science and Technology* 23 (085108).
- [2] D. E. Davison, S. J. Cornelius, N. Collings, K. Glover, Observations of trans-stoichiometric AFR spikes in UEGO sensors, *SAE Technical Papers* (2000-01-2837).

- [3] D. R. Baker, M. W. Verbrugge, Mathematical analysis of potentiometric oxygen sensors for combustion-gas streams, *AIChE Journal* 40 (9) (1994) 1498–1514.
- [4] J.-H. Lee, Review on zirconia air-fuel ratio sensors for automotive applications, *Journal of Materials Science* 38 (21) (2003) 4247–4257.
- [5] S. T. Regitz, An ultra fast Air-to-Fuel measurement device for cyclic combustion analysis, Ph.D. thesis, Cambridge University, 2009.
- [6] A. D. Brailsford, M. Yussouff, E. M. Logothetis, Theory of gas sensors, *Sensors and Actuators: B* 13 (1-3) (1993) 135–138.
- [7] T. S. Auckenthaler, C. H. Onder, H. P. Geering, Modelling of a solid-electrolyte oxygen sensor, *SAE Technical Papers* (2002-01-1293).
- [8] M. P. Hörlein, A. K. Opitz, J. Fleig, On the variability of oxygen exchange kinetics of platinum model electrodes on yttria stabilized zirconia, *Solid State Ionics* 247-248 (2013) 56–65.
- [9] J. L. Gland, Molecular and atomic adsorption of oxygen on the Pt(111) and Pt(S)-12(111)×(111) surfaces, *Surface Science* (93) (1980) 487–514.
- [10] J. L. Gland, B. A. Sexton, G. B. Fisher, Oxygen interactions with the Pt(111) surface, *Surface Science* (95) (1980) 587–602.
- [11] R. Gorte, L. D. Schmidt, Desorption kinetics with precursor intermediates, *Surface Science* (76) (1978) 559–573.
- [12] A. Mitterdorfer, L. J. Gauckler, Reaction kinetics of the Pt, O₂(g) |c-ZrO₂ system: precursor-mediated adsorption, *Solid State Ionics* 120 (1) (1999) 211–225.
- [13] S. K. Ratkje, K. S. Forland, The Transported Entropy of Oxygen Ion in Yttria-Stabilized Zirconia, *Journal of The Electrochemical Society* 138 (8) (1991) 2374–2376.

- [14] L. L. Melo, A. R. Vaz, M. C. Salvadori, M. Cattani, Grain sizes and surface roughness in platinum and gold thin films, *Journal of Metastable and Nanocrystalline Materials* 20-21 (2004) 623–628.
- [15] B. E. Poling, J. M. Prausnitz, J. P. O’Connell, *The Properties of Gases and Liquids*, McGraw-Hill, 5th edn., 2001.

Acknowledgements

The work undertaken was funded by the Engineering and Physical Sciences Research Council.

Simulation Parameters

Nomenclature

T	Temperature (K)
c_i	Concentration of species i
p	Pressure (Pa)
r	radial coordinate
X_i	Mole fraction of species i
E	Electrical potential
\mathbf{E}	Electric field
i	Electrical current

Constants

\mathfrak{R}	Molecular Gas Constant	$8314.41 \text{ J.kmol}^{-1}.\text{K}^{-1}$	
F	Faraday constant	$9.648 \times 10^7 \text{ C.kmol}^{-1}$	
Γ	Density of adsorption sites on Pt surface	$1.6603 \times 10^{-8} \text{ kmol.m}^{-2}$	[12]
τ	Diffusion barrier tortuosity	1.5	[1]
d_p	Diffusion barrier pore diameter	$1.85 \mu\text{m}$	[1]

Gas transport in the diffusion barrier [1]

M_i ($O_2 \rightarrow 32, N_2 \rightarrow 28$)	Molecular mass of species i
$A_A = \left(\frac{1}{A_C} + \frac{1}{A_K}\right)^{-1}$	Pressure drop coefficient
$D_{i,j} = \left(\frac{1}{D_{C_{i,j}}} + \frac{1}{D_{K_i}}\right)^{-1}$	Diffusivity of species i in j
$A_C = \frac{\mathfrak{R}T}{p} \frac{32\mu}{d_p^2 \sum_i (X_i M_i^{0.5})}$	Continuum pressure drop
$A_K = \frac{3}{2d_p} \sqrt{\frac{\pi \mathfrak{R}T}{2}}$	Free molecular pressure drop
$D_{C_{i,j}} = \frac{0.0101325 T^{1.75} \sqrt{1/M_i + 1/M_j}}{p (\nu_i^{1/3} + \nu_j^{1/3})^2}$	Continuum diffusivity
$D_{K_i} = \frac{d_p}{3} \sqrt{\frac{8\mathfrak{R}T}{\pi M_i}}$	Free molecular 'diffusivity'
$Sc = 0.7$	Schmidt number for gas
ν_i ($O_2 \rightarrow 16.3, N_2 \rightarrow 18.5$)	Diffusion volume of species i [15]

Oxygen adsorption to the Pt surface in equation 8. [12]

θ	Fractional coverage of oxygen on Pt surface sites
$\mathcal{F}_{O_2} = \frac{p_{O_2}}{\sqrt{2\pi M_{O_2} \mathfrak{R}T}}$	Molecular flux onto surface
$\zeta = 0.18 \exp(-14.1\theta)$	Sticking probability
$k = 0.05 \exp\left(\frac{(4 - 5\theta) \times 10^6}{\mathfrak{R}T}\right)$	Adsorbed molecular decomposition to desorption rate ratio
$k_d = 5 \times 10^{12} \exp\left(\frac{-(240 - 50\theta) \times 10^6}{\mathfrak{R}T}\right)$	Adsorbed atomic oxygen desorption rate (s^{-1})

John Harris is an EPSRC funded PhD student at Cambridge University Engineering Department, whose research is focussed on the electrochemical limitations of internal combustion engine sensors.

Professor Collings is a Member of the Staff of Cambridge University Engineering Department and is Head of the Acoustics, Fluid Mechanics, Turbomachinery and Thermodynamics Division. Professor Collings' areas of research are: the internal combustion engine and the sentient vehicle.

Accepted Manuscript